Using 25GbE Client Rates to Access the Gains of Adaptive Bit- and Code- Rate Networking

David J. Ives, Paul Wright, Andrew Lord and Seb J. Savory

***Abstract*—For transmission within optical mesh networks different signal routes acquire different impairments and are received with different SNR. The SNR can be utilised through adaptive bit- and code- rate modulation which leads to data rates that are not multiples of the preferred 100GbE client rate. This paper considers the use of slower 25GbE lanes both with inverse multiplexed 100GbE client rates and with native 25GbE client rates and compares the network blocking performance. The use of inverse multiplexed 100GbE client data onto four 25GbE lanes accesses the lions share of stranded capacity within the network.**

***Index Terms*—Optical Networking; Adaptive modulation; Blocking Probability.**

I. Introduction

With the ever increasing amount of traffic on the internet there is an urgent need to maximise the load carried by a given optical fibre infrastructure. To this end the available network resources of bandwidth and transmitted signal SNR must be fully utilised. In a wavelength routed optical network signals travel a variety of distances and routes and experience a variety of impairments leading to different signal SNRs. Thus the theoretical maximum error free spectral efficiency varies across the network. Contemporary networking has client side data rates that are fixed, for example following the Ethernet standard with 100GbE client data rates such that transport networks are designed to transport multiples of 100 $\text{Gb}\cdot\text{s}^{-1}$ client data.

The variety of transmitted signal SNRs can be fully utilised with adaptive modulation and adaptive FEC coding [1]–[5] or alternatively the signal launch power can be adapted to effectively transfer SNR margin between channels to fit the required SNR of an adapted modulation, fixed FEC coding scheme with 100GbE granularity [6]. The later requires more complex routing and wavelength assignment algorithms [7] and may not be suitable for sequential or dynamically loaded networks. The former leads to a variety of spectral efficiencies. Elastic bandwidth and flexible grids [8]–[11] could be used to maintain a fixed client rate by adjusting the symbol rate for a given spectral efficiency but this again leads to more complex routing and wavelength assignment and the difficulties of stranded bandwidth.

So we consider the simpler paradigm of a fixed optical grid, fixed optimised launch power and use an adapted modulation and adaptive FEC overhead leading to a variety of data rates. The use of a fixed grid simplifies the routing and wavelength assignment as each DWDM channel is now separately constrained. The fixed optimised launch power is obtained for the worst case, the central channel on a fully loaded network. This allows the nonlinear interference to be estimated without knowledge of the future network state [12] and ensures that the established light paths will not be blocked by the acceptance of future demands. The use of the fixed optical grid allows a small improvement in worst case nonlinear interference, with respect to a flexible grid, as the position of the guard bands are known. For a flexible grid the worst case nonlinear interference would need to be estimated based on a constant power spectral density without guard bands.

Thus in general the optimal data rate will not align with the preferred 100GbE client side rate leaving stranded capacity. As pointed out in [13] a flexible Ethernet is required to better match client and optical layers. The recent debates within IEEE 802.3 and the ethernet community suggest that 25GbE is a useful data rate that can be transported over single electrical or OOK optical channels [14], [15]. So to more fully utilise the available data rates of adaptive modulation and adaptive FEC overhead we consider inverse multiplexing the fixed 100GbE client rate onto four 25GbE lanes and transmitting these on the available unused capacity of multiple transceivers.

In this work we simulate the sequential loading of the BT 20+2 node UK core network and compare;

1) fixed PM-16QAM modulation and fixed FEC overhead transceivers accepting 2 off 100GbE client demands,
2) adaptive PM-mQAM modulation with fixed FEC overhead transceivers accepting multiple 100GbE client demands in full,
3) adaptive PM-mQAM modulation with adaptive FEC overhead transceivers with 25GbE lanes with 100GbE client demands inverse multiplexed onto 25GbE lanes and accepted on a single or across multiple transceivers,
4) adaptive PM-mQAM modulation with adaptive FEC overhead transceivers with multiple 25GbE client demands accepted in full.

These transceiver options are illustrated in figure 1. The final option is included to take full advantage of the finer granularity and is expected to show the best performance. We compare these options on blocking performance and on the number of transceivers required to transport a given network load. We also suggest how the transceiver options must be priced in order to economically increase the data transmission within the network considered here.

II. Impairment adaptive modulation and coding

We consider a network using polarization multiplexed coherent optical communications such that linear impairments are equalised in the receiver and signal transmission quality

Manuscript received Month dd, yyyy; revised Month dd, yyyy.

D. Ives (e-mail: di231@cam.ac.uk) and S. Savory were with the Optical Networks Group, Department of Electronic and Electrical Engineering, University College London, London, WC1E 7JE, UK. and are now with the Electrical Engineering Division, Department of Engineering, University of Cambridge, 9 JJ Thomson Avenue, Cambridge, CB3 0FA, UK.

A. Lord and P. Wright are with British Telecommunication core networks research, Adastral Park, Martlesham Heath, Ipswich, IP5 3RE, UK.

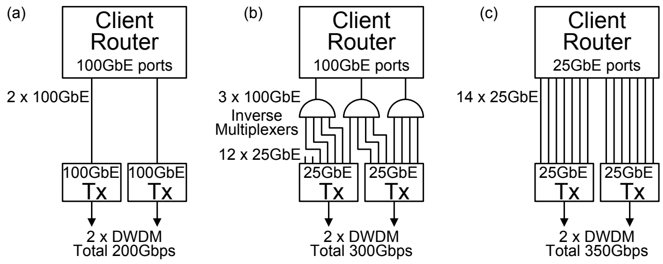

Fig. 1. Illustration of the transceiver hardware connection options considered. (a) is used with simulation options 1) and 2), (b) is used with simulation option 3) and (c) with simulation option 4).

is limited by ASE noise and nonlinear interference, NLI. We assume that NLI can be calculated using the incoherent GN model [16] and consider an Egalitarian operation [12] where all the DWDM channels are assumed equally power loaded, and the NLI of the worst case central DWDM channel is assumed for all DWDM channels. The transmission signal symbol SNR can be written as

$$SNR = \frac{p}{\sum_i ASE_i + p^3 \sum_j X(L_j)} \tag{1}$$

where p is the signal launch power of each DWDM channel, ASE_i is the ASE noise power from the i^{th} EDFA, and $X(L_j)$ is a NLI factor describing the NLI on the worst case central DWDM channel for the j^{th} span of length, L_j. All the noise powers are measured within the receivers' matched filter bandwidth. The summation i and j are over all EDFAs and fibre spans respectively, along the optical transmission route.

The ASE noise within the receivers' matched filter bandwidth is given by

$$ASE_i = 10^{\frac{NF}{10}} h\nu 10^{\frac{A_i}{10}} R \tag{2}$$

where NF is the amplifier noise figure, taken as 4.5 dB, h is Plank's constant, ν is the optical carrier frequency 193.5 THz, R is the symbol rate (Baud) and A_i is the loss between the $(i-1)^{\text{th}}$ and the i^{th} amplifier (dB) which will be fully compensated by the i^{th} amplifier. The EDFA were assumed to be equally spaced within a link with a maximum spacing of 60 km. All the ROADM nodes were assumed to have 22 dB loss compensated by a following EDFA.

$X(L)$ was obtained by numerical integration of the GN model over the full c-band, 100 channels spaced at 50 GHz and across the channel matched filter, $H(f)$. $X(L)$ is given by

$$X(L) = \frac{16}{27}\gamma^2 \int_{-\infty}^{\infty}\int_{-\infty}^{\infty}\int_{-\infty}^{\infty} g(f_1)g(f_2)g(f_1+f_2-f)H(f) \frac{1+e^{-2\alpha L} - 2e^{-\alpha L}\cos\left[4\pi^2\beta_2(f_1-f)(f_2-f)L\right]}{\alpha^2 + \left[4\pi^2\beta_2(f_1-f)(f_2-f)\right]^2}\, df_1\, df_2\, df \tag{3}$$

where the spans were assumed to be SSMF with attenuation 0.25 dB·km^{-1}, α = 0.0576 km^{-1}, chromatic dispersion 16.7 ps·nm^{-1}·km^{-1}, β_2 = -21.3 ps^2·km^{-1} and nonlinear coefficient, γ = 1.3 W^{-1}·km^{-1}. The total signal power spectral density is given by $p \times g(f)$ where the normalised power spectral density, $g(f)$, is given by

$$g(f) = \frac{1}{R}\sum_{i=-50}^{49} \text{rect}\left(\frac{f + i * \Delta f}{R}\right) \tag{4}$$

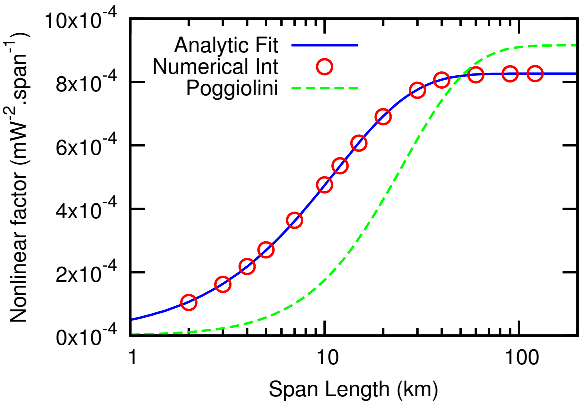

Fig. 2. Graph of nonlinear interference factor X(L) vs span length.

where R is the symbol rate of 32 GBaud, Δf the DWDM channel spacing of 50 GHz and $\text{rect}(x)$ is the rectangle function such that $\text{rect}(x) = 1$ for $-0.5 < x < 0.5$ and 0 elsewhere. The matched filter $H(f)$ is given by

$$H(f) = \text{rect}\left(\frac{f}{R}\right). \tag{5}$$

For the BT 20+2 node UK core network of figure 4 the span lengths vary considerably and thus an analytic estimation of $X(L)$ was developed to accurately capture the span length dependence and avoid repeated numerical integration, as

$$X(L) = X(\infty)\left[1 - e^{a_0 L}\right]^{a_1} \tag{6}$$

where $X(\infty) = 8.26231 \times 10^{-4}$ mW^2·span^{-1} is the NLI factor for an infinite long span obtained by numerical integration of the GN model and a_0 and a_1 where found to be 0.0987595 km^{-1} and 1.190506 respectively by fitting the numerical data to minimize the sum of squares of the error between the analytic equation and the numerical results. The numerically integrated and analytical estimation of $X(L)$ are compared in figure 2 where the RMS difference was found to be 1.3×10^{-6} mW^{-2}·span^{-1}. Also shown in figure 2 is the analytical GN model of Poggiolini [17, equation (39)] illustrating that while this is within 0.5 dB of the numerical integrated values for long span lengths there is a large discrepancy at shorter span lengths.

For a given symbol SNR the modulation format and FEC overhead were chosen to maximise the data throughput. We consider ideal hard decision FEC where for a pre-FEC BER, P_b, the maximum code rate, r_c, that results in error free transmission is given by [18]

$$r_c = 1 + P_b \log_2[P_b] + (1 - P_b)\log_2[1 - P_b] \tag{7}$$

such that for PM-QPSK modulation at 32 GBaud the maximum error free information rate is $32 \times 4 \times r_c$ Gb·s^{-1}. We allow a 5 % overhead for the OTU framing leading to a maximum client data rate $\frac{1}{1.05} 32 \times 4 \times r_c$ Gb·s^{-1} for the PM-QPSK modulation.

We actually solve the reverse of this, that is for a given data rate choose the modulation format and FEC overhead to minimise the required SNR for error free transmission. The data rates are chosen to be in multiples of 25GbE with 5 % framing OH, giving a data rate granularity of 26.25 Gb·s^{-1}. So for each modulation format the required code rate can be calculated thence from equation (7) the required pre-FEC BER, P_b can be found and finally the required SNR

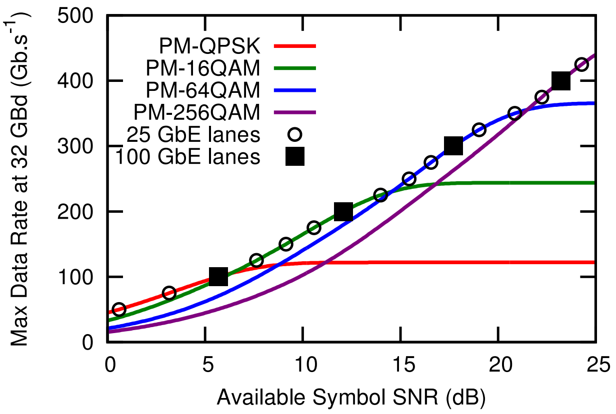

Fig. 3. Graph of client data rate versus symbol SNR for various code rate and modulation formats.

TABLE I
MODULATION FORMATS, DATA RATES AND REQUIRED SYMBOL SNRS FOR THE 32GBAUD SIGNALS USED.

Modulation Format	Code Rate	Information (Gb·s^{-1})	Client Data (Gb·s^{-1})	Required SNR (dB)
PM-QPSK	0.41	52.5	50	0.59
PM-QPSK	0.62	78.8	75	3.16
PM-QPSK	0.82	105.0	100	5.69
PM-16QAM	0.49	131.3	125	7.63
PM-16QAM	0.62	157.5	150	9.14
PM-16QAM	0.72	183.8	175	10.58
PM-16QAM	0.82	210.0	200	12.08
PM-16QAM	0.92	236.3	225	14.06
PM-64QAM	0.68	262.5	250	15.45
PM-64QAM	0.75	288.8	275	16.57
PM-64QAM	0.82	315.0	300	17.73
PM-64QAM	0.89	341.3	325	19.07
PM-64QAM	0.96	367.5	350	20.85
PM-256QAM	0.77	393.8	375	22.24
PM-256QAM	0.82	420.0	400	23.23
PM-256QAM	0.87	446.3	425	24.29
PM-256QAM	0.92	472.5	450	25.53

to achieve this pre-FEC BER can be calculated given the modulation format. The required SNR for client data rates on 100 and 25 Gb·s^{-1} lanes transported using PM-QPSK, PM-16QAM, PM-64QAM and PM-256QAM are shown in table I and illustrated in figure 3.

III. SEQUENTIAL LOADED NETWORK SIMULATIONS

To demonstrate the gains by fully utilising the available SNR, sequential loading of the BT 20+2 node UK core network was considered. Figure 4 shows the network topology and link lengths used. The subset of modulation format / code rate combinations utilised in a given network depends on the range of SNR for the light paths within that network [19] . Larger diameter networks will utilise a subset of lower data rate combinations while smaller diameter networks will use higher data rate combinations. For both cases the granularity of the data rate with SNR is 25 Gb·s^{-1} and it is the advantage of the finer granularity which this work explores and thus similar conclusions are expected for other networks.

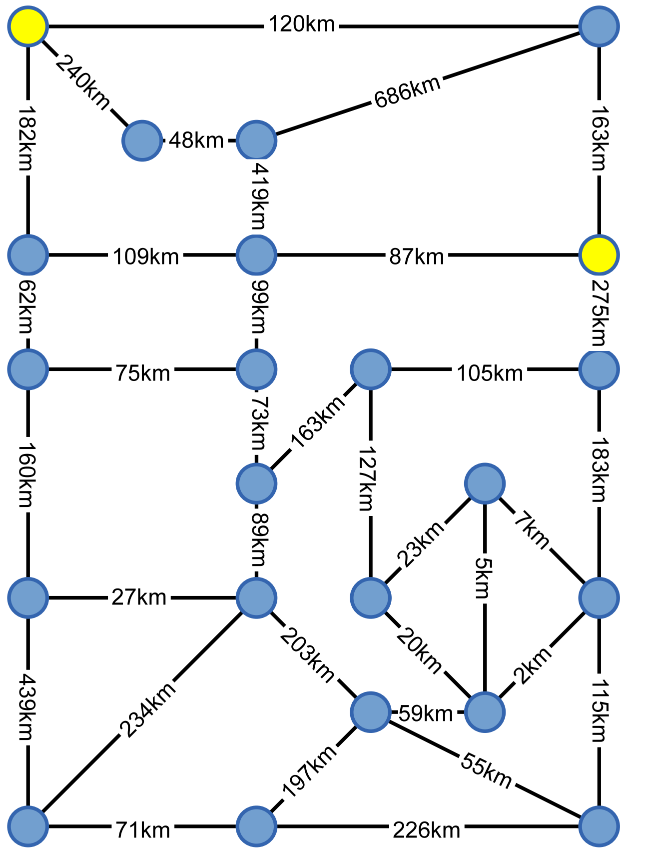

Fig. 4. The BT 20+2 node UK core topology showing link lengths in (km). The two yellow nodes did not supply or receive traffic and are for routing purposes only.

Uniformly random demands were sequentially added to the network in the following way. If a transceiver with sufficient unused capacity was available between the source and destination nodes then the demand was accepted in full by that transceiver. If a transceiver was available between the source and destination nodes with insufficient unused capacity to fully accept the demand and a new transceiver can be set up following the same path the demand was accepted across the two transceivers. Otherwise a new lightpath was routed using the congestion aware shortest path (number of hops) based on [18] and if DWDM spectrum was available the first fit wavelength chosen to activate the transceiver. The SNR of the available route was calculated and the highest capacity signal format chosen from Table I where the route SNR exceeds the required SNR for error free transmission. The demand was accepted onto the new transceiver. If all these options fail then the demand was deemed to have been blocked. The process of routing and accepting a demand is illustrated in the flow chart of figure 5.

Either 2000, 100 Gb·s^{-1} or 8000, 25 Gb·s^{-1} bi-directional demands, a total of 400 Tb·s^{-1}, were imposed on the network and the accumulation of blocking and number of active transceivers recorded. The simulation was repeated 10000 times and the mean accumulated blocking calculated to improve the statistics. The cumulative blocking probability after the i^{th} demand was calculated as, CBP_i,

$$\text{CBP}_i = \frac{\text{Block}_i}{i} \tag{8}$$

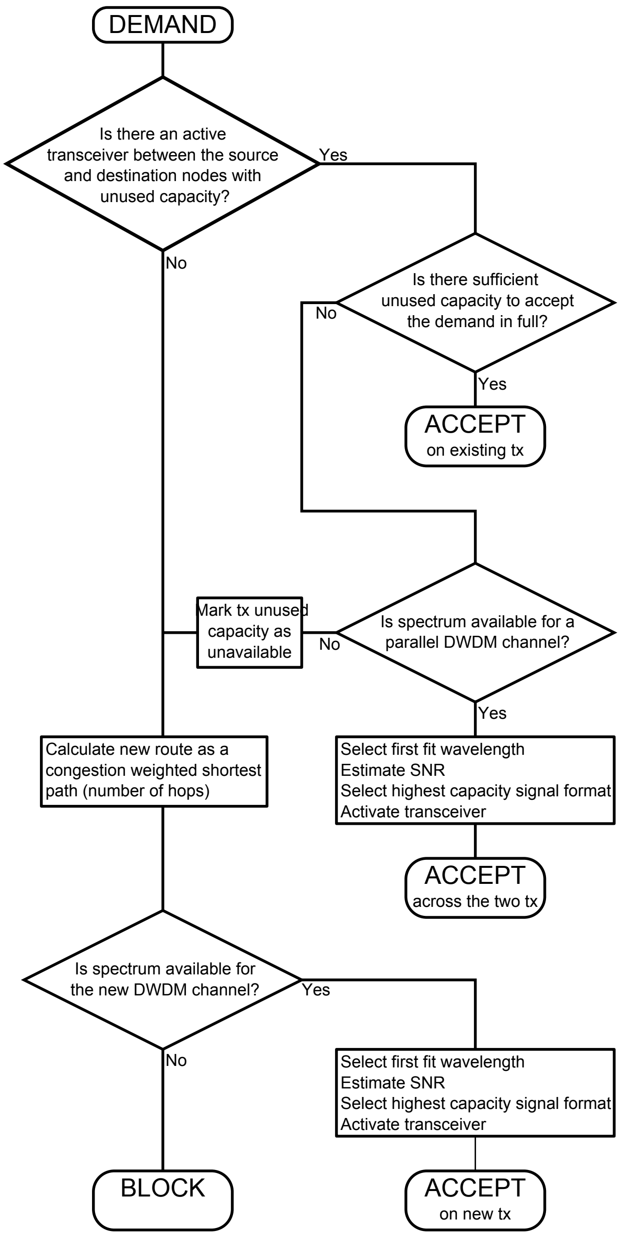

Fig. 5. The process of routing and accepting sequential demands.

where Block_i is the mean accumulated blocking after the i^{th} demand. The mean accepted network load after the i^{th} demand is thus $i(1 - \text{CBP}_i)$ and the probability that the next demand will be blocked, BP_i was calculated from the cumulative blocking probability as

$$\text{BP}_i = (i+1)\ \text{CBP}_{i+1} - i\ \text{CBP}_i. \tag{9}$$

The network load that gives a 1 % blocking probability was calculated by linearly fitting the blocking probability versus load in the log domain over a blocking probability range of 0.5 % to 2 %. The 0.1 % and 10 % blocking probabilities were also calculated by fitting over 0.05 % to 0.2 % and 6 % to 15 % respectively.

The simulation was carried out for four different sets of transceiver and demand profiles: for a fixed 200 Gb·s^{-1} PM-16QAM modulation format accepting upto 2 off 100GbE demands, for an adapted PM-mQAM modulation format with fixed FEC overhead giving 100 Gb·s^{-1} client data granularity and accepting multiple 100GbE demands in full, for an adapted PM-mQAM modulation format with adapted FEC overhead giving 25 Gb·s^{-1} client data granularity with the 100GbE demands inverse multiplexed across four 25GbE lanes and accepted across single or multiple transceivers and for an adapted format PM-mQAM with adapted FEC overhead giving 25 Gb·s^{-1} client data granularity with the multiple 25GbE demands accepted in full. Figure 1 illustrates the transceiver configuration options.

TABLE II
NETWORK LOAD FOR A NUMBER OF BLOCKING PROBABILITIES AND THE NUMBER OF ACTIVE TRANSCEIVERS AT A NETWORK LOAD OF 200 TB·S^{-1} FOR THE FOUR TRANSCEIVER CONFIGURATIONS CONSIDERED.

Transceiver Configuration	Network Load (Tb·s^{-1}) for blocking probability			No. Tx at load
	0.1 %	1 %	10 %	200 Tb·s^{-1}
Fixed PM-16QAM Fixed FEC-OH 100GbE demands	206.4	213.3	223.4	1095
Adaptive PM-mQAM Fixed FEC-OH 100GbE demands	224.8	232.1	243.1	913
Adaptive PM-mQAM Adaptive FEC-OH 100GbE demand	251.4	265.1	280.7	854
Adaptive PM-mQAM Adaptive FEC-OH 25GbE demands	266.9	273.3	290.0	861

Figure 6 shows the blocking probability versus accepted load for the different transceiver configurations described above. The network load at 0.1 %, 1 % and 10 % blocking probabilities are shown in table II and increase from 213.3 to 273.3 Tb·s^{-1} for 1 % blocking in going from fixed PM-16QAM modulation with fixed FEC overhead and 100GbE demands to adapted PM-mQAM modulation with adapted FEC overhead and 25GbE demands. For transceivers with 100GbE client data granularity the stranded capacity will range from 0 to <100 Gb·s^{-1} and thus it is expected that on average 50 Gb·s^{-1} per transceiver of client data capacity will be stranded by incomplete utilisation of the available SNR. Given that approximate 1000 transceivers are active then 50 Tb·s^{-1} of client data capacity is unused. This stranded capacity will fall to an average of 50 Gb·s^{-1} per node pair when the demands are inverse multiplexed onto 25GbE lanes, a total of 19 Tb·s^{-1} and fall further to 12.5 Gb·s^{-1} per transceiver when 25GbE client demands are used a total of just 12.5 Tb·s^{-1}. This view is consistent with the results shown in figure 6 and suggests that moving to 100GbE demands split across four 25GbE lanes gives the lions share of capacity improvement.

Figure 7 shows the evolution of the number of active transceivers in the network as the network load is increased for the four different transceiver configurations. The point at which 0.1 %, 1 % and 10 % blocking probabilities occur are marked by triangle, circle and square symbols respectively. It

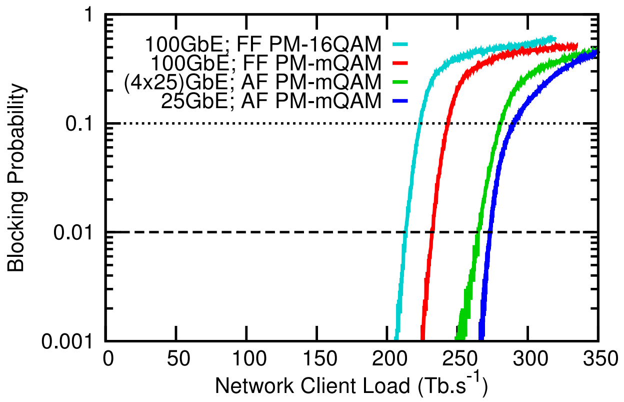

Fig. 6. Blocking probability versus network load for the BT 20+2 node UK core network. For the four transceiver configurations considered, FF = fixed FEC-OH, AF = adaptive FEC-OH.

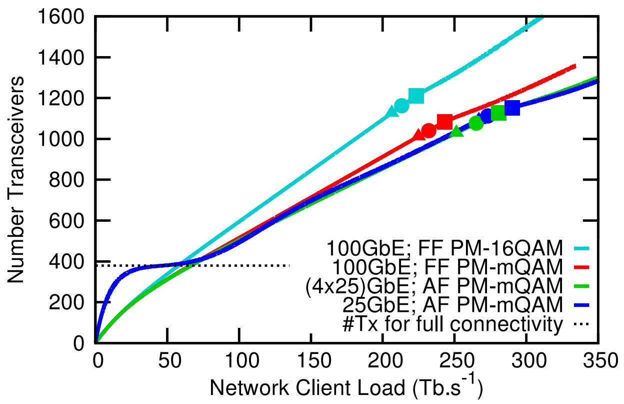

Fig. 7. Number of active transceivers versus network load for the BT 20+2 node UK core network. For the four transceiver configurations considered, FF = fixed FEC-OH, AF = adaptive FEC-OH. The triangle, circle and square symbols correspond to blocking probabilities of 0.1 %, 1 % and 10 % respectively. The dotted line indicates 380 transceivers, the minimum required to fully connect the network.

can be seen that by using adaptive modulation and adaptive FEC overhead fewer transceivers are required at the higher network loads. It also shows that at higher loads 100GbE demands split across four 25GbE lanes utilises approximately the same number of transceivers as using 25GbE demands directly but suffers slightly earlier blocking. At low network loads the use of 25GbE demands shows significantly more transceivers are required for a given network load. Near zero load the number of transceivers required increases with the number of demands such that for 25GbE demands the number of transceivers will increase four times faster than for 100GbE demands by a given load. This initial rise continues until there are 380 transceivers, enough to fully connect the network and then the unused capacity on transceivers is used to accommodate further demands leading to a plateau in the number of transceivers required. This low load regime is not an area of interest for future optical networking.

By comparing the number of transceivers used at the higher network load of 200 Tb·s^{-1} it is possible to estimate the break even economic price for the different transceiver technologies. The final column of table II shows the average number of transceivers used to accept the load of 200 Tb·s^{-1} under the four different transceiver configurations considered. For the technology to be economically acceptable then the price of including adaptive format technology needs to be less than 20 % greater than a fixed PM-16QAM transceiver and the price of including adaptive FEC overhead should not increase the transceiver price by more than 6 % above that of a fixed FEC coded adaptive modulation transceiver. This final 6 % must also include the cost of any electronic switches required to convert the 100 GbE signals into multiple 25GbE signals and connect them to multiple transceivers.

IV. Conclusions

This paper has considered the problem of fully utilising the available SNR resource in a sequentially loaded mesh network. The use of adaptive modulation formats and adaptive FEC overhead can access the available capacity but leads to transceiver capacities that are not multiples of the currently preferred client data rate.

We show through sequential loading of the BT 20+2 node UK core network that by inverse multiplexing 100GbE demands onto four 25GbE lanes that can be split across multiple transceivers the majority of the stranded capacity can be utilised.

We also compare the number of transceivers required to support a given network load and conclude that for such technologies to be economically viable, within the BT 20+2 node UK core network, the adaptive modulation format capable transceivers must cost no more than 20 % more than fixed PM-16QAM transceivers and the adaptive FEC overhead must add no more than 6 % to the price of adaptive modulation format capable transceivers.

Acknowledgements

The authors would like to acknowledge the support from the UK EPSRC through the project grant INSIGHT, EP/L026155/1 and the programme grant UNLOC, EP/J017582/1, The Royal Academy of Engineering / The Leverhulme Trust and also from the EU seventh framework programme through the IDEALIST project no. 317999.

References

[1] G.-H. Gho and J. M. Kahn, “Rate-Adaptive Modulation and Coding for Optical Fiber Transmission Systems,” *Journal of Lightwave Technology*, vol. 30, no. 12, pp. 1818–1828, Jun. 2012. [Online]. Available: http://ieeexplore.ieee.org/lpdocs/epic03/wrapper.htm?arnumber=6159047

[2] M. Arabaci, I. B. Djordjevic, L. Xu, and T. Wang, “Nonbinary LDPC-Coded Modulation for Rate-Adaptive Optical Fiber Communication Without Bandwidth Expansion,” *IEEE Photonics Technology Letters*, vol. 24, no. 16, pp. 1402–1404, Aug. 2012. [Online]. Available: http://ieeexplore.ieee.org/lpdocs/epic03/wrapper.htm?arnumber=6218753

[3] L. Potì, G. Meloni, G. Berrettini, F. Fresi, M. Secondini, T. Foggi, and G. Colavolpe, “Casting 1 Tb/s DP-QPSK Communication into 200 GHz Bandwidth,” in *European Conference on Optical Communication*, Brussels (BE), 2012, p. P4.19.

[4] D. A. A. Mello, A. N. Barreto, T. C. de Lima, T. F. Portela, L. Beygi, and J. M. Kahn, “Optical Networking With Variable-Code-Rate Transceivers,” *Journal of Lightwave Technology*, vol. 32, no. 2, pp. 257–266, Jan. 2014. [Online]. Available: http://ieeexplore.ieee.org/lpdocs/epic03/wrapper.htm?arnumber=6674043

[5] A. Alvarado, D. J. Ives, S. J. Savory, and P. Bayvel, “On Optimal Modulation and FEC Overhead for Future Optical Networks,” in *Optical Fiber Communication Conference*, vol. 12. Los Angeles, CA. (USA): OSA, 2015, p. Th3E.1. [Online]. Available: http://www.opticsinfobase.org/abstract.cfm?URI=OFC-2015-Th3E.1

[6] D. J. Ives, P. Bayvel, and S. J. Savory, "Assessment of Options for Utilizing SNR Margin to Increase Network Data Throughput," in *Optical Fiber Communication Conference*. Los Angeles, CA. (USA), Mar. 2015, p. M2I.3. [Online]. Available: http://www.opticsinfobase.org/abstract.cfm?URI=OFC-2015-M2I.3

[7] ——, "Physical Layer Transmitter and Routing Optimization to Maximize the Traffic Throughput of a Nonlinear Optical Mesh Network," in *Optical Network Design and Modeling*, Stockholm (SE), May 2014, pp. 168–173. [Online]. Available: http://ieeexplore.ieee.org/xpl/login.jsp?arnumber=6855789

[8] M. Jinno, H. Takara, B. Kozicki, Y. Tsukishima, Y. Sone, and S. Matsuoka, "Spectrum-efficient and scalable elastic optical path network: architecture, benefits, and enabling technologies," *IEEE Communications Magazine*, vol. 47, no. 11, pp. 66–73, Nov. 2009. [Online]. Available: http://ieeexplore.ieee.org/lpdocs/epic03/wrapper.htm?arnumber=5307468

[9] O. Gerstel, M. Jinno, A. Lord, and S. J. B. Yoo, "Elastic optical networking: a new dawn for the optical layer?" *IEEE Communications Magazine*, vol. 50, no. 2, pp. s12–s20, Feb. 2012. [Online]. Available: http://ieeexplore.ieee.org/lpdocs/epic03/wrapper.htm?arnumber=6146481

[10] F. Fresi, "Self-Adaptation Technique for Bandwidth-Variable Transponders," in *Photonics in Switching*, 2015, pp. 157159.

[11] F. Cugini, F. Paolucci, F. Fresi, G. Meloni, N. Sambo, L. Potì, A, D'Errico, and P. Castoldi "Toward Plug-and-Play Software-Defined Elastic Optical Networks." *Journal of Lightwave Technology*, vol. 34, no. 6, pp. 14941500, Mar. 2016. [Online]. Available: http://doi.org/10.1109/JLT.2015.2511802

[12] D. J. Ives, A. Lord, P. Wright, and S. J. Savory, "Quantifying the Impact of Non-linear Impairments on Blocking Load in Elastic Optical Networks," in *Optical Fiber Communication Conference*, no. 1, San Francisco, CA. (USA), Mar. 2014, p. W2A.55.

[13] X. Zhao, V. Vusirikala, B. Koley, V. Kamalov, and T. Hofmeister, "The prospect of inter-data-center optical networks," *IEEE Communications Magazine*, vol. 51, no. 9, pp. 32–38, Sep. 2013. [Online]. Available: http://ieeexplore.ieee.org/lpdocs/epic03/wrapper.htm?arnumber=6588647

[14] *25 Gb/s Ethernet Task Force*, IEEE Std. [Online]. Available: http://www.ieee802.org/3/by

[15] *25G Ethernet Consortium*, Std. [Online]. Available: http://25gethernet.org

[16] P. Poggiolini, "The GN Model of Non-Linear Propagation in Uncompensated Coherent Optical Systems," *Journal of Lightwave Technology*, vol. 30, no. 24, pp. 3857–3879, Dec. 2012. [Online]. Available: http://ieeexplore.ieee.org/lpdocs/epic03/wrapper.htm?arnumber=6296670

[17] P. Poggiolini, "The GN-Model of Fiber Non-Linear Propagation and its Applications," *Journal of Lightwave Technology*, vol. 32, no. 4, pp. 694–721, Feb. 2014. [Online]. Available: http://ieeexplore.ieee.org/lpdocs/epic03/wrapper.htm?arnumber=6685826

[18] S. J. Savory, "Congestion Aware Routing in Nonlinear Elastic Optical Networks," *IEEE Photonics Technology Letters*, vol. 26, no. 10, pp. 1057–1060, May 2014. [Online]. Available: http://ieeexplore.ieee.org/lpdocs/epic03/wrapper.htm?arnumber=6781032

[19] A. Alvarado, D. J. Ives, S. J. Savory, and P. Bayvel "On the Impact of Optimal Modulation and FEC Overhead on Future Optical Networks.," *Journal of Lightwave Technology*, vol. 34, no. 9, pp. 2339–2352, May 2016. [Online]. Available: http://jlt.osa.org/abstract.cfm?URI=jlt-34-9-2339